



# Preliminary safety analysis for heavy water-moderated molten salt reactor

Gao-Ang Wen<sup>1</sup> · Jian-Hui Wu<sup>2,3</sup> · Chun-Yan Zou<sup>2,3</sup> · Xiang-Zhou Cai<sup>2,3</sup> · Jin-Gen Chen<sup>2,3</sup> · Man Bao<sup>1</sup>

Received: 8 October 2023 / Revised: 23 January 2024 / Accepted: 19 February 2024 / Published online: 18 June 2024

© The Author(s), under exclusive licence to China Science Publishing & Media Ltd. (Science Press), Shanghai Institute of Applied Physics, the Chinese Academy of Sciences, Chinese Nuclear Society 2024

## Abstract

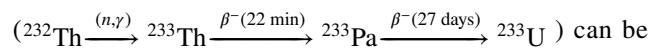
The heavy water-moderated molten salt reactor (HWMSR) is a newly proposed reactor concept, in which heavy water is adopted as the moderator and molten salt dissolved with fissile and fertile elements is used as the fuel. Issues arising from graphite in traditional molten salt reactors, including the positive temperature coefficient and management of highly radioactive spent graphite waste, can be addressed using the HWMSR. Until now, research on the HWMSR has been centered on the core design and nuclear fuel cycle to explore the viability of the HWMSR and its advantages in fuel utilization. However, the core safety of the HWMSR has not been extensively studied. Therefore, we evaluate typical accidents in a small modular HWMSR, including fuel salt inlet temperature overcooling and overheating accidents, fuel salt inlet flow rate decrease, heavy water inlet temperature overcooling accidents, and heavy water inlet mass flow rate decrease accidents, based on a neutronics and thermal–hydraulics coupled code. The results demonstrated that the core maintained safety during the investigated accidents.

**Keywords** Heavy water-moderated molten salt reactor · Neutronics and thermal–hydraulics coupling · Transient analysis · Accident analysis

## 1 Introduction

Molten salt reactors (MSRs) use fluoride/chloride salts dissolved with fissile and fertile fuel elements as fuel. During core operation, liquid fuel continuously circulates through the primary loop of the MSRs. Online reprocessing has become viable, through which soluble fission products

(FPs) can be removed online and valuable heavy metal elements can be recycled online. Online helium bubbling can also be used to remove soluble fission products. Superior performance in terms of safety, neutronics, and fuel utilization can be achieved in an MSR compared with solid fuel reactors. Most importantly, the intermediate isotope, Pa-233, in the reaction chain as Th-232 converts to U-233



can be extracted online outside the core to decay to U-233. Thus, the neutron absorption of Pa-233 in the core can be significantly reduced. Hence, MSRs are considered most suitable for thorium utilization.

The feasibility and safety of MSRs have been demonstrated by the successful operation of the Molten Salt Reactor Experiment (MSRE) designed and built by the Oak Ridge National Laboratory (ORNL), USA, in the 1960s [1]. Since then, China (1970s), the Soviet Union (1970s), Japan (1980s), and the European Union (1980 s) have begun to engage in technology development and the conceptual design of MSRs [1, 2]. However, most of these MSR research activities were terminated because of the lack of

This work was supported by the National Natural Science Foundation of China (No.11905285), the Shanghai Natural Science Foundation (No. 20ZR1468700), and the Youth Innovation Promotion Association CAS (No.2022258).

✉ Jian-Hui Wu  
wujianhui@sinap.ac.cn

✉ Man Bao  
mbao@usst.edu.cn

<sup>1</sup> College of Science, University of Shanghai for Science and Technology, Shanghai 200093, China

<sup>2</sup> Shanghai Institute of Applied Physics, Chinese Academy of Sciences, Shanghai 201800, China

<sup>3</sup> University of Chinese Academy of Sciences, Beijing 100049, China

national-level program support against the background of the nuclear industry depression in the 1980–1990s. This situation improved in the 2000s because the MSR was selected as a candidate for the six GEN-IV advanced reactors in 2002 [3] and many innovative concepts for small modular MSRs have been proposed [4]. Notably, in 2011, the Chinese Academy of Sciences (CAS) initiated the Thorium Molten Salt Reactor (TMSR) nuclear energy system project with the aim of achieving the efficient utilization of thorium for energy production and hydrogen generation within the next 20–30 years [2]. Many studies related to the TMSR have been conducted by the CAS [5–12].

Most of the conceptual MSR designs, as introduced above, belong to graphite-moderated MSRs, in which graphite with high temperature and corrosion resistance is used as the moderator, and fuel channels are constructed, allowing fuel salt to flow through the core. The results of existing research on graphite-moderated MSRs demonstrate their advantages in terms of the fuel cycle and safety; however, some studies have shown that graphite-moderated MSRs are limited by the use of graphite [13]. One of these limitations is the positive temperature coefficient caused by graphite heating, which leads to neutron spectrum hardening and subsequently favors the fission of U-233 over the capture of Th-232 [14, 15]. High-performance preparation technologies are required for graphite to prevent the permeation of fuel and Xe-135 and result in a large change in the core reactivity. Furthermore, graphite must be replaced periodically because of neutron irradiation damage at high operational temperatures. Approximately 272 tons of highly radioactive spent graphite must be replaced for a 1000-MWe molten salt breeder reactor (MSBR) every four years, and most importantly, an effective approach has not been designed for the disposal of highly radioactive spent graphite. The use of isotopically enriched carbon (up to 99.9% C-12) may minimize long-term radioactive waste; however, the high cost of producing enriched carbon remains an issue. Although research conducted by Li *et al.* [16] indicates that a negative temperature reactivity coefficient may be achieved for graphite by adjusting the core geometric parameters, the management of highly radioactive graphite remains a great challenge.

Recently, several MSR concepts have been proposed using different moderators such as lead, ZrH<sub>4</sub>, and BeO [17] to address the issues associated with graphite. However, these alternatives have disadvantages. For example, solid moderators such as ZrH<sub>4</sub> and BeO require periodic replacement owing to neutron irradiation. Another effective method is to replace graphite with heavy water as a moderator. In 2013, researchers from the Los Alamos National Laboratory proposed a salt-cooled modular thorium reactor system [18]. The system uses heavy water as the moderator and thorium as fuel and is considered safer and more

sustainable for thorium utilization compared to traditional solid fuel reactors.

Heavy water is an excellent moderator and was adopted by the Canada Deuterium Uranium (CANDU) reactor. It has the highest neutron moderation capability (ratio of neutron moderation to absorption cross section, 2100 [19]) among existing moderators, approximately 12 times that of graphite. Using heavy water as the moderator would significantly benefit both the neutron economy and nuclear fuel cycle [20]. Most importantly, heavy water can be efficiently purified online and recycled via a heavy water reprocessing system, as in the CANDU reactor. Thus, the disposal of highly radioactive spent graphite in graphite-moderated MSRs can be addressed. However, heavy water can extend the time of neutron moderation and diffusion compared with graphite, which can retard the peak of core reactivity and mitigate the fluctuation of core reactivity in an accident. Using heavy water as a moderator also has the additional advantage of generating photoneutrons, which can increase the effective delayed neutron fraction and enhance reactor safety margins. Hence, safer operation can be expected for heavy water-moderated MSRs (HWMSRs) [19].

Until now, HWMSRs have been extensively studied in terms of core design and fuel cycle since it was proposed in 2019 by Wu *et al.* [19]. In their study, superior performance of the thorium–uranium fuel cycle was observed compared with that in graphite-moderated MSRs. In 2022, Wu *et al.* conducted a study on the transition to a thorium fuel cycle in a 1000 MWe low enriched uranium (LEU)-started HWMSR core using various scenarios, including different U-235 enrichment and reprocessing times (RTs). The results demonstrated that the transition to a thorium fuel cycle can be achieved by loading the LEU with 19.75 wt% U-235/U enrichment no lower than 5% in the HWMSR, which is impossible in a graphite-moderated MSR owing to inferior neutron economics [21]. The influences of the reprocessing cycle time and reprocessing separation efficiency on the core actinide inventory evolution, breeding ratio (BR), and nuclear waste radiotoxicity were also investigated in subsequent studies [21]. Considering the significant advantages of neutronics, the utilization of natural uranium (NU) in HWMSR was explored by Wu *et al.* [21]. The results revealed that the fuel utilization efficiency can reach 1%, which marginally surpassed that of the CANDU reactor. In addition, approximately 2262 kg of U-233 can be produced over 20 years of operation via online thorium refueling and Pa-233 extraction, which is sufficient for starting three new thorium-fueled HWMSR cores [22]. In addition to large power-scale HWMSRs, research activities on core design and the nuclear fuel cycle in a 530-MWth small modular HWMSR (SM-HWMSR) were also conducted by Zhang *et al.* [23].

As mentioned above, the HWMSR provides considerable advantages in the nuclear fuel cycle, but it must be evaluated within the framework of safety guidelines, which have not yet

been considered. In view of the higher realizability of small modular reactors (SMRs) compared with large power-scale reactors, owing to the low construction cost and core siting flexibility of SMRs [24], this study conducts a safety evaluation for a 530-MWth SM-HWMSR. Transients with a high occurrence frequency, including molten salt overcooling and overheating, fuel salt flow rate decrease, heavy water overcooling, and heavy water mass flow rate decrease, are preliminarily evaluated to demonstrate the safety of HWMSRs.

## 2 Overview of the SM-HWMSR system

The SM-HWMSR analyzed in this study adopts fluoride molten salt dissolved with fission and fertile elements as the fuel and heavy water as the moderator. It has a thermal power of 530 MW, and the fission energy in the core is transferred by two loops, as shown in Fig. 1 [25]. The primary loop operates at ambient pressure and functions to safely transfer the fission energy to the secondary loop; it comprises the core, control rod system, and moderator cooling system. Fuel salt conduits are regularly arranged in the core to separate the high-temperature fuel salt (600 °C) from the low-temperature heavy water moderator (60 °C). The fission energy released in the fuel salt is carried out from the core by the fuel salt flowing through the conduits and is then transferred to the secondary loop in the intermediary heat exchanger. Control rods installed in the core are used to regulate core reactivity and shut down the reactor core during accidents. Molten salt drain tanks below the core allow fuel salt to be quickly

discharged from the core by gravity in case of an emergency. An online fuel reprocessing system was applied to remove sparingly soluble FPs, including fission gas and noble metals, and to recycle useful heavy metal elements.

To prevent the heavy water from boiling, an excellent thermal insulator, 8YSZ-50% (8 mol%  $Y_2O_3/92$  mol%  $ZrO_2$ , sintered into porous spheres with a relative density of 50%), was applied to the wall of the fuel salt conduit to minimize the heat transfer between the fuel salt and heavy water [26, 27]. According to the analysis conducted by Wu et al., a 3 mm thickness of 8YSZ-50% is sufficient to maintain the temperature of heavy water below boiling point, which was adopted in this study. Moreover, two SiC layers with a thickness of 0.5 mm were placed inside and outside the 8YSZ-50% insulator layer to resist corrosion from both the fuel salt and heavy water [28]. A heavy water recycling system was adopted to remove the deposited heat resulting from gamma and neutron irradiation and the heat transferred from the fuel salt.

The core design of the SM-HWMSR is illustrated in Fig. 2. Both the fuel salt and moderator have negative temperature reactivity coefficients of (−1.125 pcm/K) and (−3.635 pcm/K), respectively. In addition, a deep negative void fraction coefficient of the moderator (−60 pcm/%) is presented. The inlet temperatures for the fuel salt and heavy water were set to 600 °C and 60 °C, respectively, based on the designs of the TMSR and CANDU reactors [19, 26]. A flow rate of 1.8 m<sup>3</sup>/s was used for the fuel salt with reference to that of the MSBR [29]. The HWMSR is a liquid-fueled reactor in which fissile elements are dissolved in molten salt, serving as both fuel and coolant. Effective multiplication can be

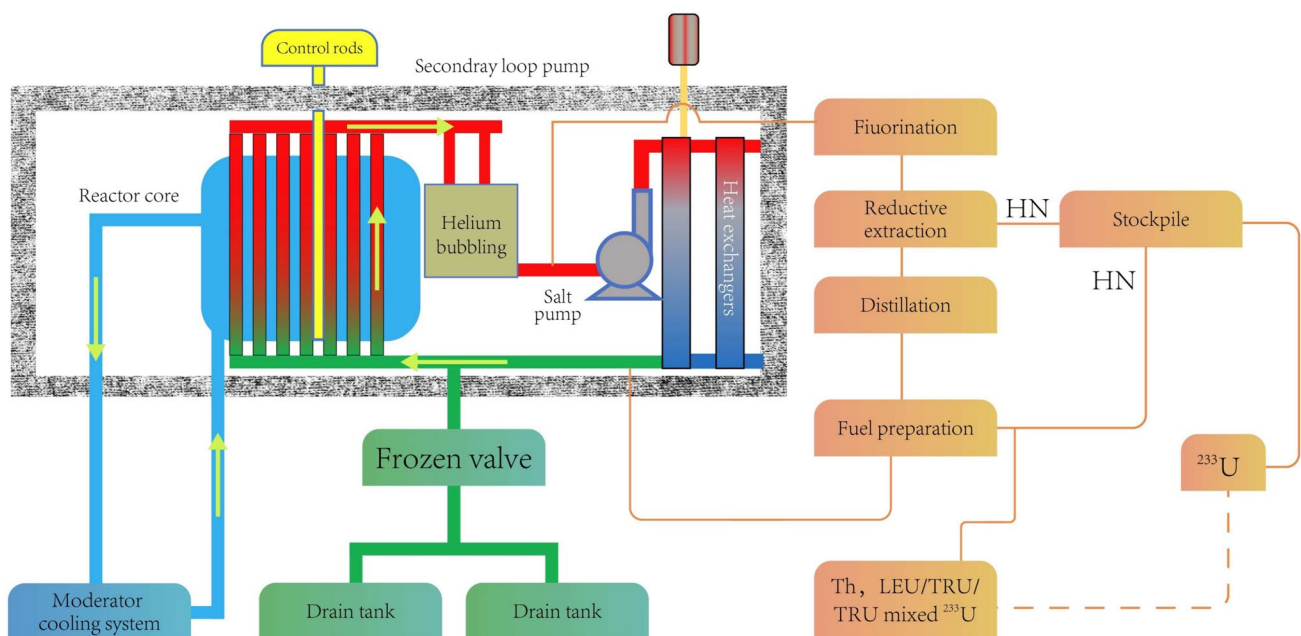
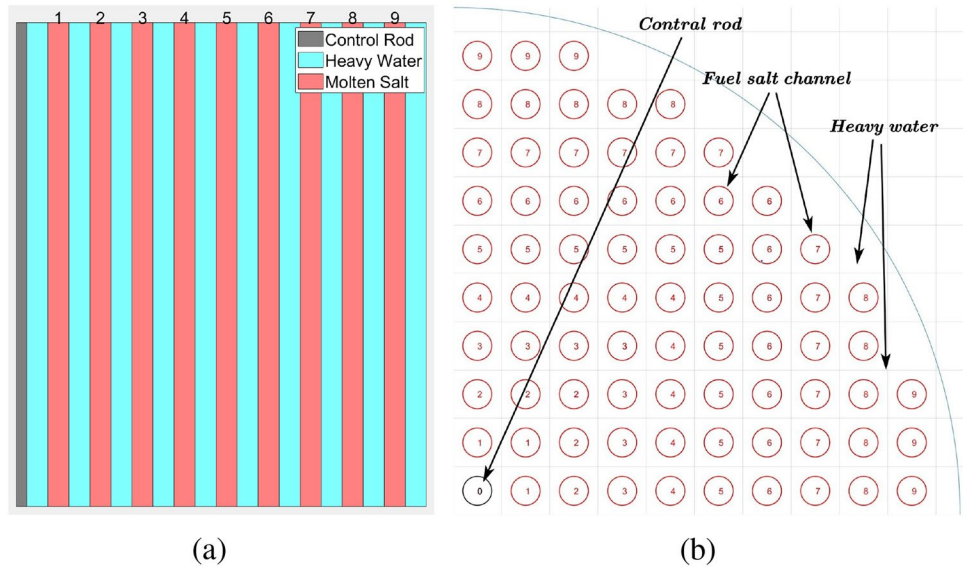


Fig. 1 (Color online) Outline of SM-HWMSR system

**Fig. 2** (Color online) **a** Multi-channel model for SM-HWMSR; **b** cross section of quarter core



**Table 1** Specification of main parameters for SM-HWMSR

Parameter	Value
Core power (MWth)	530
Core inlet temperature of fuel salt (°C)	600
Core outlet temperature of fuel salt (°C)	650
Inlet temperature of heavy water (°C)	60
Outlet temperature of heavy water (°C)	62
Inlet mass flow rate of fuel salt (kg/s)	4.7
Heavy water velocity (m/s)	0.6
Radius of active core (m)	1.89
Height of active core (m)	3.78
Number of fuel channels	267
Thickness of SiC (mm)	0.5
Thickness of insulator (mm)	3

adjusted online by feeding liquid fuel, allowing it to remain at approximately 1 throughout the fuel cycle [19]. Considering this, effective multiplication was not investigated in this study. Effective multiplication can be adjusted online by feeding the liquid fuel, allowing it to remain at approximately 1 throughout the fuel cycle. The specific core and physical property parameters of the fuel salt and heavy water are summarized in Tables 1 and 2, respectively.

### 3 Neutronic–thermohydraulic coupling calculations

As in graphite-moderated MSRs, neutronics tightly couples with the thermal hydraulics in SM-HWMSRs owing to the application of liquid fuel, in which the released fission energy is directly absorbed. A more rapid temperature

response to power changes was observed in the core compared with solid fuel reactors. Moreover, delayed neutron precursors (DNPs) entrained in the flowing fuel salt continuously circulate through the primary loop, influencing the transient behavior of the core during accidents. The calculation of the distribution of DNPs should consider the velocity of the fuel salt [30, 31]. The temperature distribution of heavy water is another issue unique to the SM-HWMSR and should be addressed by coupling the core power and fuel salt temperature. In this study, an in-house two-dimensional dynamics code specialized for HWMSR (HWMSR-2D) was developed based on the TMSR-2D, which is a dynamic calculation code designed for graphite-moderated MSRs [32–35], by replacing graphite with flowing heavy water.

### 3.1 Neutron kinetic model

Neutron kinetics is an important indicator of core safety and is defined as the behavior of spatial neutron flux over time. In this study, two-group time-dependent neutron diffusion equations, in which the delayed neutrons are considered as fast group neutrons, are employed for modeling the neutron kinetics of the SM-HWMSR:

$$\frac{1}{V_1} \frac{\partial \phi_1}{\partial t} = \nabla \cdot (D_1 \nabla \phi_1) + (1 - \beta)(\nu \Sigma_{f1} \phi_1 + \nu \Sigma_{f2} \phi_2) - \Sigma_{t1} \phi_1 + \sum_{i=1}^6 \lambda_i C_i, \tag{1}$$

$$\frac{1}{V_2} \frac{\partial \phi_2}{\partial t} = \nabla \cdot (D_2 \nabla \phi_2) - \Sigma_{t2} \phi_2 + \Sigma_{1 \rightarrow 2} \phi_1, \tag{2}$$

**Table 2** Composition and physical property parameters for the molten salts and heavy water [19, 31]

Parameter	Value
Fuel salt composition (mol%)	LiF–BeF <sub>2</sub> –ThF <sub>4</sub> –UF <sub>4</sub> 71.7% LiF–16% BeF <sub>2</sub> –12.3% HNF <sub>4</sub>
Coolant salt composition (second loop) (mol%)	LiF–NaF–KF 46.5%LiF–11.5%NaF–42%KF
Fuel salt specific heat capacity (J/kg · K)	1985
Fuel salt density (kg/m <sup>3</sup> )	3.153 – 5.925 08 × 10 <sup>-4</sup> T
Fuel salt viscosity coefficient (Pa · s)	8.8
Fuel salt thermal conductivity (W/m · K)	0.4461 + 0.0005T
Boiling point of fuel salt (K)	1676
Thermal feedback coefficients of fuel salt (pcm/K)	-1.125
Heavy water density (kg/m <sup>3</sup> )	1.1
Heavy water specific heat capacity (J/kg · K)	4187
Heavy water thermal conductivity (W/m · K)	0.668
Heavy water viscosity coefficient (Pa · s)	0.419
Thermal feedback coefficients of heavy water (pcm/K)	-3.635
Allowable temperature of heavy water (K)	373
Fuel salt friction coefficient	
<i>Re</i> ≤ 3000	<i>f</i> = 64/ <i>Re</i>
<i>Re</i> > 3000	<i>f</i> = 0.3164/ <i>Re</i> <sup>0.25</sup>
Fuel salt Nusselt number	
<i>Re</i> ≤ 3000	<i>Nu</i> = 1.62( <i>RePrL/H</i> ) <sup>0.33</sup>
<i>Re</i> > 3000	<i>Nu</i> = 0.23 <i>Re</i> <sup>0.8</sup> <i>Pr</i> <sup>0.33</sup>
SiC thermal conductivity (W/m · K)	370
Insulator thermal conductivity (W/m · K)	0.7514 – 0.0017T + 2 × 10 <sup>-6</sup> T <sup>2</sup> – 1 × 10 <sup>-9</sup> T <sup>3</sup>

where subscripts 1 and 2 represent the fast and thermal neutron groups, respectively,  $\phi$  is the neutron flux,  $V$  represents the neutron velocities,  $\Sigma_f$  and  $\Sigma_t$  represent the fission and neutron absorption cross sections, respectively,  $D$  represents the diffusion coefficient,  $\Sigma_{1 \rightarrow 2}$  indicates the transfer cross section from the fast neutron group to the thermal group,  $\nu$  represents the number of neutrons produced per fission, and  $\beta$  represents the total fraction of delayed neutrons.

During the core operation of the SM-HWMSR, the fuel salt continuously circulates in the primary loop at a velocity of 0.8 m/s. The flow effect of the fuel salt on the neutron flux could be neglected because of the significantly higher velocity of the neutron flux in the core. However, this should be considered for DNP kinetics because the flow of the fuel salt causes the DNP to flow out of the core and subsequently reduce the fraction of delayed neutrons in the core [36]. The DNP balance equations in the SM-HWMSR can be expressed as follows:

$$\frac{\partial C_i}{\partial t} = \beta_i \sum_{g=1}^2 \Sigma_{f,g}(\vec{r}) \phi_g(\vec{r}, t) - \lambda_i C_i - \frac{\partial(UC_i)}{\partial z} \quad i = 1, \dots, 6, \tag{3}$$

where  $C_i$  and  $\lambda_i$  represent the concentration and decay constants of the  $i$ -th group of DNPs, respectively, and  $U$  represents the velocity of the fuel salt. The first term on the right-hand side of Eq. (3) represents the generation of DNPs resulting from the nuclear fission reaction. The second and third terms represent the decay of the DNPs and influence of the fuel salt flow, respectively.

In general, the neutrons in different positions of the core make different contributions to the power, which is defined as the neutron importance. This can be calculated by solving the adjoint equations of the steady-state neutron flux [37]:

$$\nabla \cdot (D_1 \nabla \phi_1^\dagger) - \Sigma_{t1} \phi_1^\dagger + (1 - \beta) \nu \Sigma_{f1} (\phi_1^\dagger + \phi_2^\dagger) - \sum_{i=1}^6 \lambda_i C_i^\dagger = 0 \tag{4}$$

$$\nabla \cdot (D_2 \nabla \phi_2^\dagger) - \Sigma_{t2} \phi_2^\dagger + \Sigma_{1 \rightarrow 2} \phi_1^\dagger = 0 \tag{5}$$

$$-\frac{\partial(UC_i^\dagger)}{\partial z} = \beta_i \sum_{g=1}^2 (\nu \Sigma_{fg}) - \lambda_i C_i^\dagger, \tag{6}$$

where  $\phi_1^\dagger$ ,  $\phi_2^\dagger$ , and  $C_i^\dagger$  denote the adjoint of  $\phi_1$ ,  $\phi_2$ , and  $C_i$ , respectively. The importance of the delayed

neutrons is given by Eq. (6), which differs from that of prompt neutrons (Eqs. (4)-(5)), because the position of the DNP changes in a timely manner, and some of the DNPs decay outside the core. In addition, the effective delayed neutron fraction for group  $i$  must be weighted according to the total adjoint neutron flux, as expressed in Eq. (7):

$$\beta_{\text{eff}}^i = \frac{\sum_{n=1}^2 \int_V \phi_n^\dagger(r) \lambda_i C_i(r) dV}{\sum_{i=1}^6 \sum_{n=1}^2 \int_V \phi_n^\dagger(r) \lambda_i C_i(r) dV + (1 - \beta) \sum_{n=1}^2 \sum_{g=1}^2 \int_V \phi_n^\dagger(r) (v \Sigma_f)_g \phi_g(r) dV} \tag{7}$$

### 3.2 Thermal-hydraulics model

Because the fuel salt flows through the fuel channels without lateral interaction in the SM-HWMSR, the parallel multi-channel model is adopted to evaluate the performance of the fuel salt thermal hydraulics with the conservation of mass and momentum, expressed as follows [38]:

$$\frac{\partial W}{\partial t} = \sum_{i=1}^N \frac{\partial W_i}{\partial t}, \tag{8}$$

$$\begin{aligned} \frac{\partial}{\partial t} \left( \frac{W_i}{A_i} \right) + \frac{\partial}{\partial z} \left( \frac{W_i^2}{\rho A_i^2} \right) \\ = - \frac{\partial p}{\partial z} - \frac{f W_i^2}{2 D_i \rho A_i^2} - \rho g - \frac{\zeta W_i^2}{2 \rho A_i^2}, \end{aligned} \tag{9}$$

where  $W_i$  is the mass flow rate in the  $i$ -th channel,  $N$  is the total number of fuel salt channels,  $A_i$  is the cross-sectional area of the  $i$ -th channel,  $\rho$  is the density of the fuel salt,  $D_i$  is the diameter of the  $i$ -th channel, and  $\zeta$  is the form resistance factor. Considering that the fuel salt conduits are interconnected at both the inlet and outlet of the core, the pressure over the entire fuel salt conduit at these two points is set to be the same and is considered as a boundary condition to solve Eqs. (8)-(9).

Unlike the flow of fuel salt through the conduits, the heavy water surrounding the fuel channels connects to itself; therefore, lateral flow should be considered for the thermal-hydraulic calculation of heavy water. However, considering the small density change with temperature below the boiling point of heavy water, the lateral flow would be small; thus, it was not considered in this study. Lateral flow may be significant during severe accidents, such as fuel channel breakage, which would result in the local boiling of heavy water. These cases will be studied in the future using a coupled two-phase heavy water flow model. Considering the above, a single-channel

thermal-hydraulics model was adopted for heavy water calculations. As shown in Fig. 3, the heavy water flows through the core with the heavy water on the one side and molten salt on the other side of the fuel salt channel. The heat transferred from the molten salt to the heavy water and the energy deposited in the heavy water owing

to neutron and gamma irradiation were assumed to be removed by the heavy water circulation loop.

Considering the heat transfer between the fuel salt and heavy water, the temperature of both can be calculated based on energy conservation:

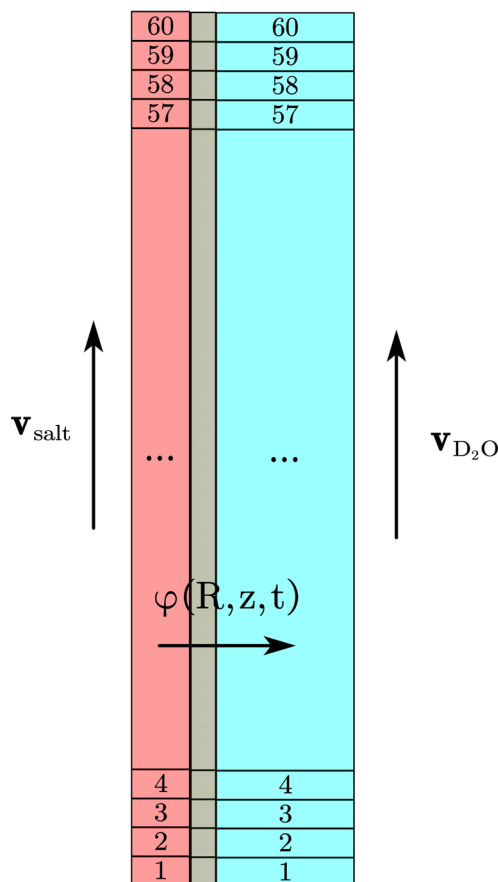


Fig. 3 (Color online) Single-channel thermal-hydraulics model for heavy water

$$\begin{aligned} \frac{\partial T_m(z, t)}{\partial t} + V_m(z, t) \frac{\partial T_m(z, t)}{\partial z} \\ = \frac{P_m(z, t)}{\pi R^2 \rho_m c_m} - \frac{\phi(R, z, t)}{\pi R^2 \rho_m c_m}, \end{aligned} \tag{10}$$

$$\begin{aligned} \frac{\partial T_D(z, t)}{\partial t} + V_D(z, t) \frac{\partial T_D(z, t)}{\partial z} \\ = \frac{P_D(z, t)}{\pi (R_p^2 - R^2) \rho_m c_m} + \frac{\phi(R, z, t)}{\pi (R_p^2 - R^2) \rho_D c_D}, \end{aligned} \tag{11}$$

where  $T_m$  is the temperature of the molten salt,  $V_m$  represents the velocity of the molten salt,  $P_m$  is the power released in the molten salt,  $\rho_m$  and  $c_m$  are the density and heat capacity of the molten salt, respectively,  $R$  is the radius of the molten salt channel,  $\phi(R, z, t)$  represents the heat flux transferred from the molten salt to the heavy water,  $T_D$  is the temperature of the heavy water,  $V_D$  is the flow velocity of the heavy water,  $P_D$  is the power deposited in the heavy water by fission,  $\rho_D$  and  $c_D$  are the density and heat capacity of the heavy water, respectively, and  $R_p$  is the equivalent radius of a single lattice.

### 3.3 Neutronics and thermal–hydraulics coupling

The macroscopic neutron cross sections of the material involved in the core are temperature-dependent parameters that should be provided before solving the neutron kinetic equations in Sect. 3.1. In this study, they were prepared using the DRAGON-4 code [39], which was developed by the Institute of Nuclear Engineering of the Polytechnic School of Montreal. The obtained macroscopic neutron cross sections were then tabulated with the temperatures of the molten salt and heavy water to couple the neutronics and thermal–hydraulics models [32]:

$$\begin{aligned} \Sigma(T_m, T_D) = AB\Sigma(T_{m2}, T_{D2}) + A(1 - B)\Sigma(T_{m2}, T_{D1}) \\ + (1 - A)B\Sigma(T_{m1}, T_{D2}) \\ + (1 - A)(1 - B)\Sigma(T_{m1}, T_{D1}) \end{aligned}, \tag{12}$$

where

$$A = \frac{T_m - T_{m1}}{T_{m2} - T_{m1}}, \quad B = \frac{T_D - T_{D1}}{T_{D2} - T_{D1}}. \tag{13}$$

As shown in Fig. 4, the HWMSR-2D code comprises three functional modules: temperature-dependent macroscopic neutron cross section preparation, steady-state calculation, and transient calculation. The temperature-dependent macroscopic neutron cross section module is first executed to provide the required macroscopic neutron cross section for the steady-state calculation, in which the neutronics and thermal

hydraulics are coupled by tabulated temperature-dependent macroscopic neutron cross sections. First, a uniform power distribution was used to obtain the initial temperature distributions of the fuel salt and heavy water and the flow rate in the fuel channels, which were then fed back to the neutronics calculations to update the power distribution. The neutronics calculation was performed using the deterministic method. This iterative calculation continued until the temperature of the molten salt converged, and the control rod position was then iteratively adjusted to ensure that the core achieved criticality. Transient calculations were conducted considering the steady-state core as the initial condition. The time-dependent N-TH coupled calculation continued until the preset time step was completed. The above processes were realized via programming using Fortran. The deterministic software DRAGON was used to perform cell neutronic calculations to provide a macroscopic cross section for the HWMSR-2D.

### 3.4 Steady-state characteristics of SM-HWMSR

The steady state of the SM-HWMSR is the starting point of the transients and should be evaluated before calculating the transients. Figure 5 shows the temperature distributions of molten salt and heavy water at the steady state with the average flow velocity of fuel salt at 0.8 m/s and that of heavy water at 0.6 m/s. The green area in the figure represents the control rod channel. The two-group neutron flux and power distributions are shown in Fig. 6, and the flow distribution of the core is shown in Fig. 7. The departure of the radial thermal neutron distribution peak from the center led to a corresponding deviation in the core power distribution. Thus, the maximum outlet temperature was located in the second and third groups of the fuel salt channels. In this study, the transversal flow of heavy water was neglected, considering the lower temperature of heavy water compared to its boiling point and the consequent marginal density difference across the core. In addition, the temperature difference of heavy water across the core was also small ( $< 3^\circ\text{C}$ ) because of the excellent heat transfer isolation of the thermal insulator. Moreover, the mass flow rate of the fuel salt within each fuel salt channel varied marginally, owing to the relatively low power peak and high heat capacity of the fuel salt. The control rod was partially inserted into the core, which enhanced the thermal neutron absorption in the core center. As the reactor power was more dependent on the distribution of thermal neutrons, the maximum power density was located in the second group of fuel salt channels rather than at the center of the core.

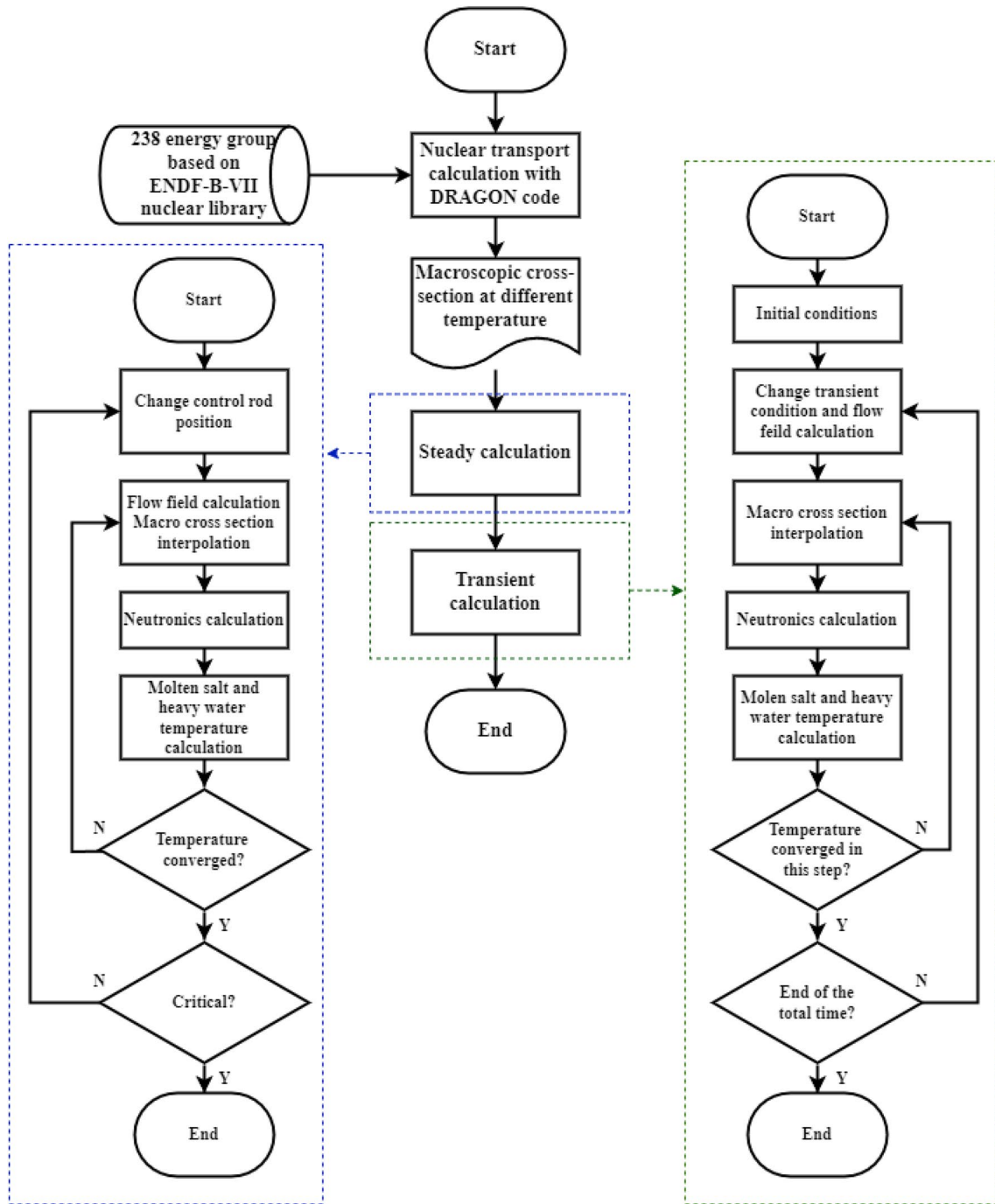


Fig. 4 Calculation flow chart of HWMSR-2D

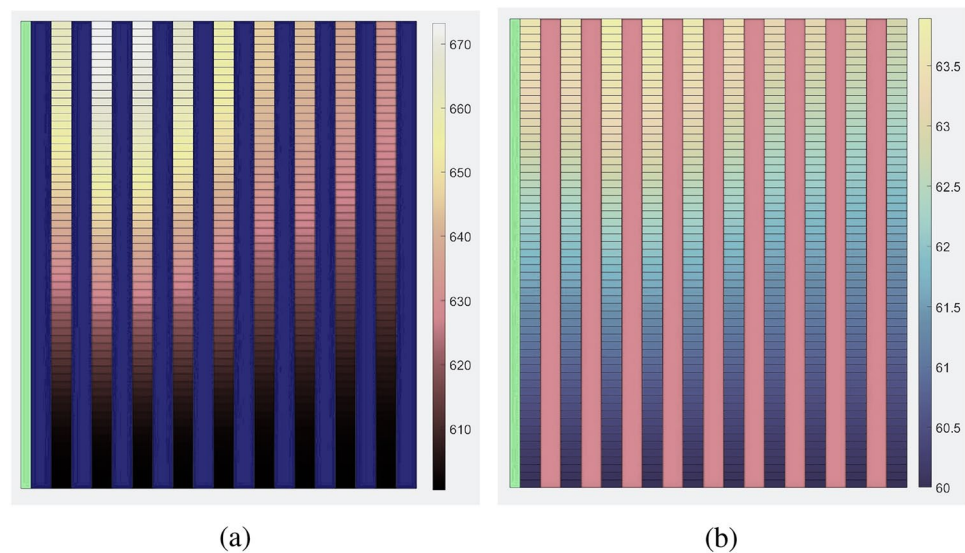
### 4 Transient accident analysis

Transients are a type of accident that is expected to occur at a high frequency over the lifetime of the core and can endanger the safety of the reactor; thus, they require extensive analysis. In the HWMSR, both the molten salt and heavy water have large negative temperature reactivity coefficients, as presented in Table 2. A small temperature

variation in either material may introduce a relatively large reactivity to the core and would cause fluctuations in core power, consequently impacting core safety. Additionally, malfunctioning of the molten salt or heavy water pumps would result in a reduction in the flow rates of the molten salt and heavy water, which in turn would increase the core temperature. Given the above considerations, this study mainly focuses on transients with a high occurrence,



**Fig. 5** (Color online) Temperature distributions of **a** molten salt and **b** heavy water



including molten salt and heavy water overcooling accidents, a flow rate decrease of molten salt, and a mass flow rate decrease of heavy water. Considering the properties of structure materials and heavy water, two limitations, i.e.,  $475\text{ }^{\circ}\text{C} < \text{fuel salt temperature} \leq 700\text{ }^{\circ}\text{C}$ , and a heavy water moderator temperature  $< 100\text{ }^{\circ}\text{C}$ , are considered to obtain the lower limit of transients for maintaining core safety.

#### 4.1 Overcooling of inlet fuel salt

Overcooling of the inlet fuel salt occurs as the external load suddenly increases or the flow rate in the second loop increases, which leads to the enhancement of heat transfer from the primary loop to the second loop. This transient is simulated by assuming that it occurs on the basis of a steady state and that the control rods remain still during the transient. Figure 8 displays the core response to a transient in which the inlet fuel temperature linearly decreased by  $60\text{ }^{\circ}\text{C}$  during 15 s, which refers to the study conducted by Cui et al., [32]. As illustrated in the figure, the core power and outlet temperature of the fuel salt gradually increased and eventually reached a new steady state owing to the positive reactivity introduced by the decrease in the fuel salt inlet temperature. Although the temperature of the heavy water increased, it was only approximately  $1\text{ }^{\circ}\text{C}$  because of the excellent heat transfer isolation of the thermal insulator, which was well within the safe range.

The outlet temperature of the fuel salt decreased and then increased at the beginning of the transient owing to the competition between the inlet temperature decline and the power increase. As the inlet temperature decreased, which introduced a positive reactivity to the core, the core power increased, leading to an increase in the outlet temperature of the fuel salt. However, this increase in the

outlet fuel salt temperature could not offset the temperature reduction resulting from the decrease in the inlet fuel salt temperature. As the inlet fuel salt temperature further decreased, which indicated that a larger temperature increase would be imposed on the core power, the increase in the outlet temperature owing to the power increase surpassed the temperature reduction resulting from the inlet temperature decrease. This resulted in a gradual increase in the outlet fuel salt temperature. The increase in the fuel salt and heavy water temperatures, in turn, introduced a negative reactivity to the core, subsequently limiting the increase in core power. Therefore, the increased power and resulting negative reactivity owing to the temperature increase compete, leading to a new steady state with a high outlet fuel salt temperature.

Figure 9 shows the responses of the core power, fuel salt outlet temperature, and heavy water outlet temperature to transients in which the inlet fuel salt temperature decreased by  $20\text{--}100\text{ }^{\circ}\text{C}$ . As demonstrated in Fig. 9a, the case in which the fuel salt inlet temperature exhibited a larger decrease resulted in a higher core power and longer time to achieve a steady state owing to the larger positive reactivity introduced to the reactor core. The increased power subsequently increased the outlet temperature of the fuel salt, as shown in Fig. 9b. Furthermore, a decrease in the inlet fuel salt temperature should not exceed  $60\text{ }^{\circ}\text{C}$  to ensure core safety (outlet fuel salt temperature  $< 700\text{ }^{\circ}\text{C}$ ). The decrease in the outlet temperature at the beginning of the transient was owing to the abrupt decrease in the inlet temperature. Moreover, the increased temperature of the fuel salt led to an increase in the heavy water temperature, but at a small scale, owing to the thermal insulation effect of the conduit wall, as shown in Fig. 9c.

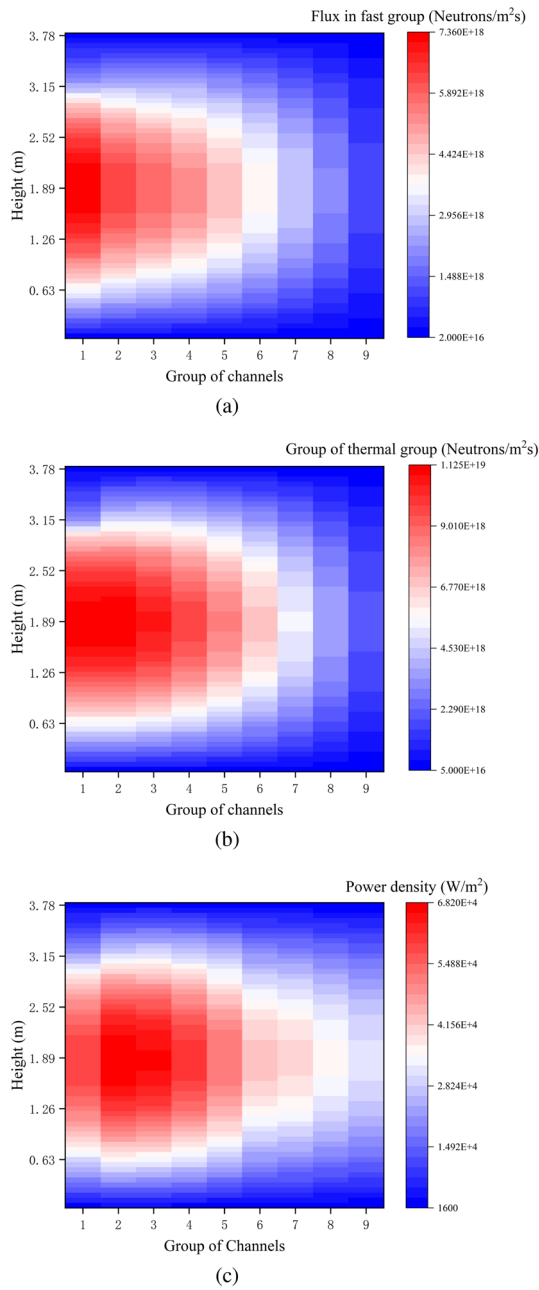


**Fig. 6** (Color online) **a, b** Distributions of neutron flux for two energy groups under steady state and **c** power density distribution of the core

## 4.2 Overheating of inlet fuel salt

Inlet fuel salt overheating occurs when the external loads suddenly decrease or the flow rate in the second loop decreases (e.g., owing to a pipe rupture in the second loop).

A 60 °C increase in the fuel salt inlet temperature triggers the frozen valve to open and discharge the fuel salt to the drain tank by gravity to ensure core safety [40];

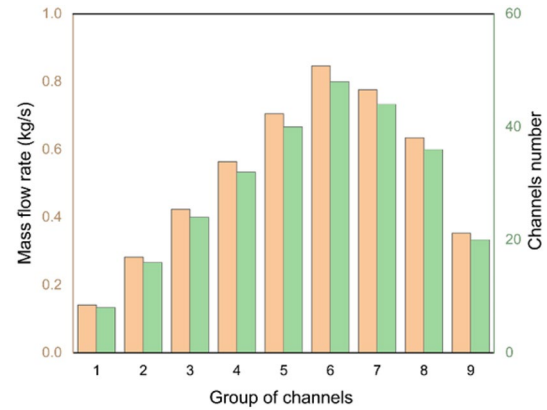


**Fig. 7** (Color online) Mass flow rate distribution in each group of channels. Orange-yellow represents fuel salt mass flow rate, and green represents the number of channels

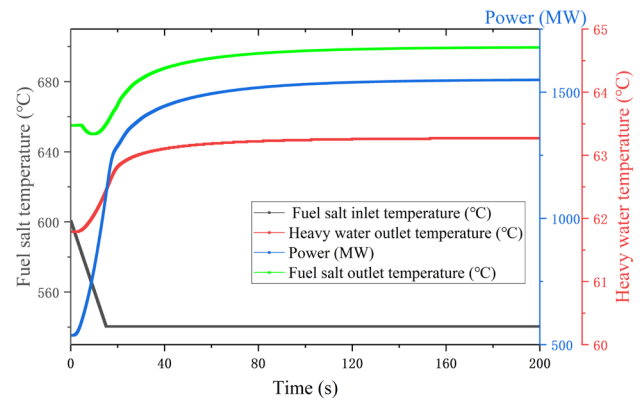


**Fig. 8** (Color online) Overcooling transient with the fuel salt inlet temperature decreased by 60 °C

therefore, a transient in which the inlet temperature of the fuel salt increases by 60 °C within 15 s was investigated to conservatively ensure core safety. Figure 10 displays the time behavior of the core power, fuel salt outlet temperature, and heavy water outlet temperature during the transient. A rapid decrease in the core power was observed at the beginning owing to the rapid increase in the inlet fuel salt temperature, which introduced a large negative reactivity to the core. A decrease in core power decreased the fuel salt outlet temperature. However, this decrease did not offset the increase resulting from the inlet temperature increase at the beginning of the transient. As the transient proceeded, the core power further decreased, which caused the fuel salt outlet temperature to gradually decrease and eventually be maintained at a value that was marginally higher than the inlet fuel salt temperature.

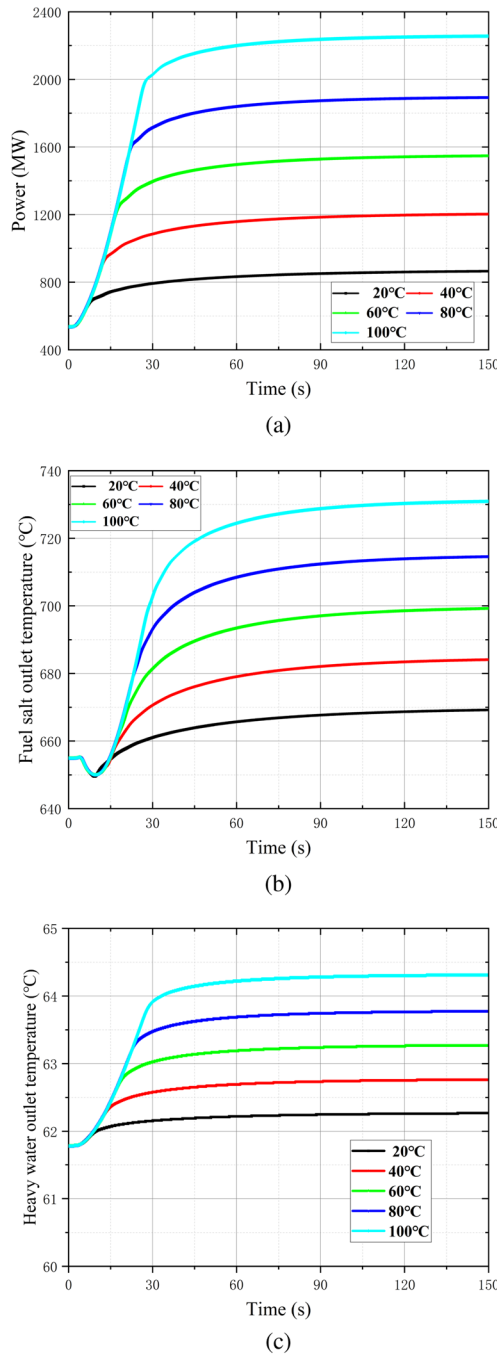


**Fig. 9** (Color online) **a** Power response, **b** fuel salt outlet temperature response, and **c** heavy water outlet temperature response to transients in which the inlet fuel salt decreased by different temperatures

### 4.3 Fuel salt flow rate decrease

The decrease in the flow rate of the inlet fuel salt is an anticipated transient for the SM-HWMSR and may be caused by a failure of or fault in the fuel salt pump. This would increase the residence time of the fuel salt in the core, causing an increase in the fuel salt temperature and

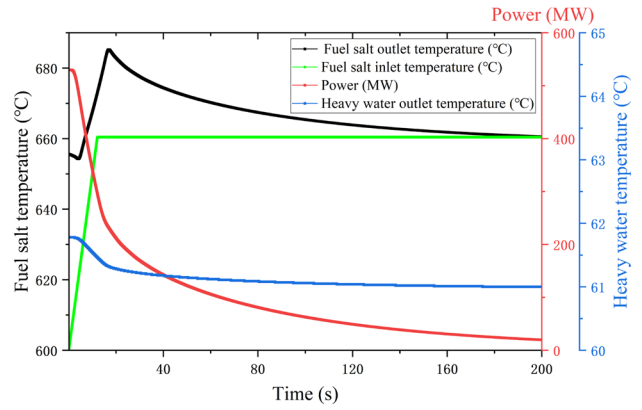


**Fig. 10** (Color online) Overheating transient in which the fuel salt inlet temperature increased by 60 °C

subsequently introducing negative reactivity to the core. However, it would mitigate the outflow of DNP from the core, resulting in an increase in core power. Figure 11 shows the responses of the core power, fuel salt outlet temperature, and heavy water outlet temperature to a transient in which the fuel salt flow rate decreased by 60% over 15 s. At the beginning of the transient, the power increased marginally owing to an increase in DNP in the core. It then decreased rapidly because of the significant temperature increase in the fuel salt, which introduced a large negative reactivity to the core. The continuous decrease in power caused a decrease in the fuel salt temperature after reaching its maximum value. Eventually, the core was balanced at a new steady state, with the fuel salt outlet temperature reaching approximately 700 °C. Periodic fluctuations in the DNP fraction in the core resulting from changes in the molten salt flow rate led to fluctuations in both the core power and fuel salt outlet temperature. Although the increased fuel salt temperature increased the heat transferred to the heavy water, the significant decrease in core power, which resulted in the reduction

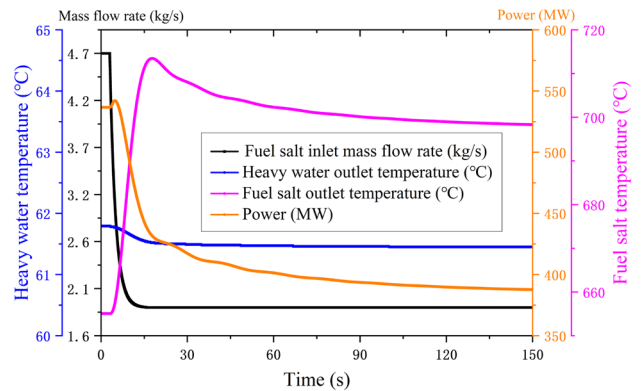


**Fig. 11** (Color online) Reactor response to a transient in which the fuel salt flow rate decreased by 60%

in radiation-induced heat deposits in the heavy water, led to a marginal decrease in the heavy water temperature, as observed in Fig. 11.

Figure 12 shows the behaviors of power and the outlet temperatures of fuel salt and heavy water during transients in which the inlet fuel salt flow rate decreased by 20–70%. The fuel salt with a more decreased flow rate resulted in a

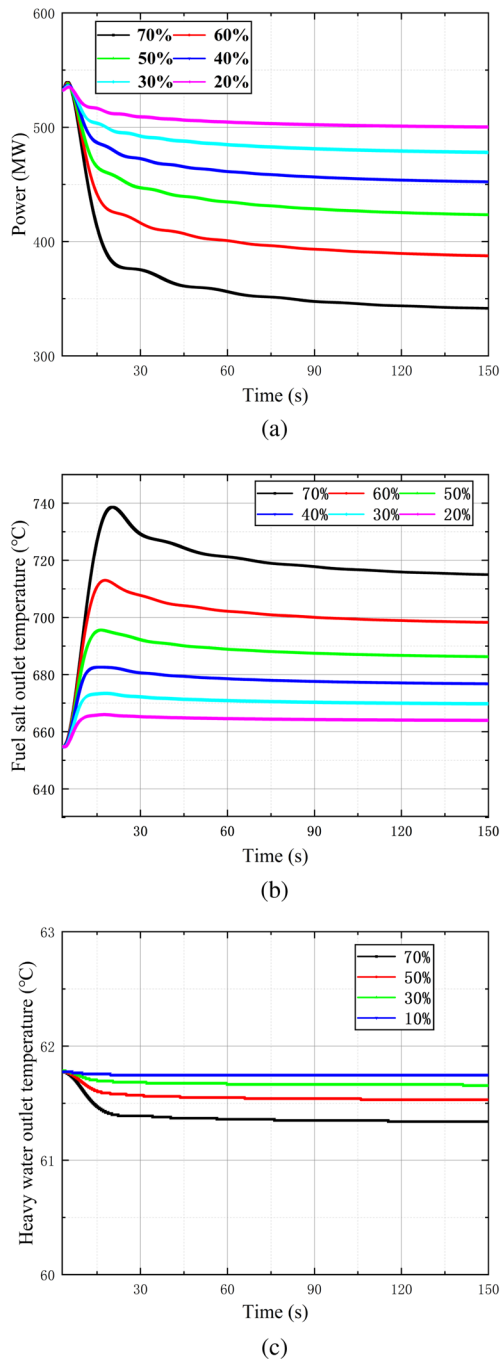


**Fig. 12** (Color online **a** Power response, **b** fuel salt outlet temperature response, and **c** heavy water outlet temperature response to transients in which the fuel salt flow rate decreased by 20–70%

longer residence time of the fuel salt in the core. This subsequently led to a higher fuel salt temperature and introduced stronger negative reactivity to the core, resulting in a lower core power. Although a change in the DNP fraction in the core affected the core power, this contribution was relatively small. As a result, the DNP fraction increase in the core for the transient with a larger decrease in fuel salt flow rates could only lead to a greater fluctuation in power, but could not change the overall decreasing trend of the core power. The decrease in the heavy water temperature increased as the flow rate of the fuel salt decreased further because the effect of the core power decrease on the heavy water temperature was stronger than that of the fuel salt temperature increase. The figures also show that the fuel salt flow rate could not decrease by more than 60% to ensure that the core temperature was lower than 700 °C.

#### 4.4 Overcooling and overheating of inlet heavy water

Heavy water has a high negative temperature coefficient of reactivity ( $-3.635$  pcm/K). Therefore, perturbation of the inlet heavy water temperature may lead to reactor accidents. Figure 13 shows a transient in which the heavy water inlet temperature decreased linearly from 60 °C to 40 °C in 10 s. The decrease in the heavy water inlet temperature led to a decrease in the bulk heavy water temperature, which subsequently resulted in an increase in reactor power owing to the introduction of positive reactivity. The increased power then caused the molten salt outlet temperature to increase, which in turn introduced negative reactivity and reduced the rate of the power increase. Eventually, the reactor reached a new steady state when the molten salt outlet temperature approached 700 °C.

Figure 14 shows the behaviors of power and the outlet temperatures of fuel salt and heavy water during transients in

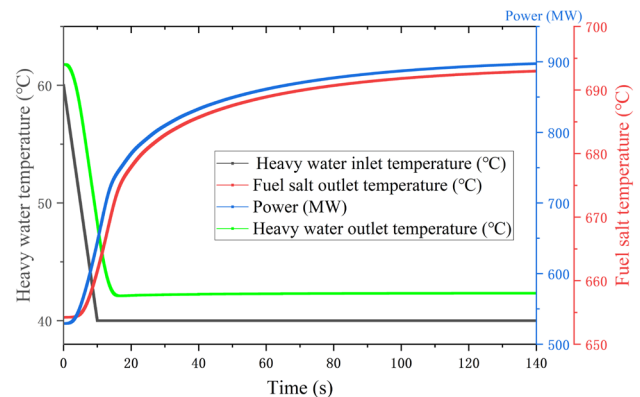
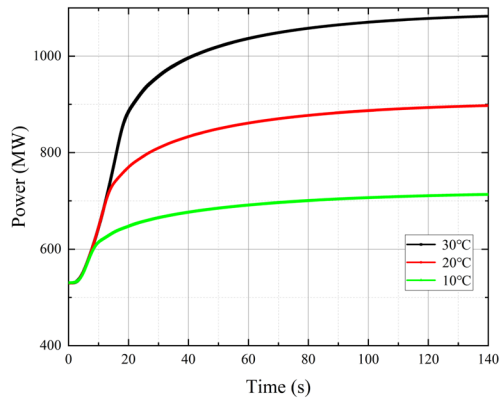
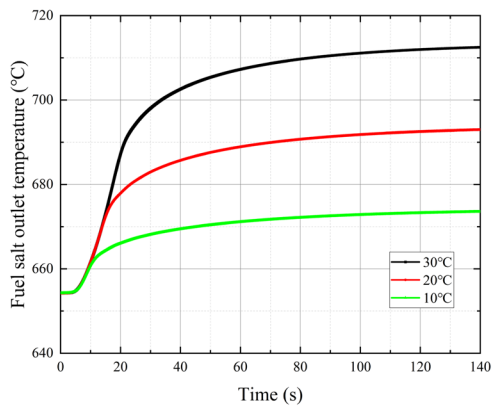


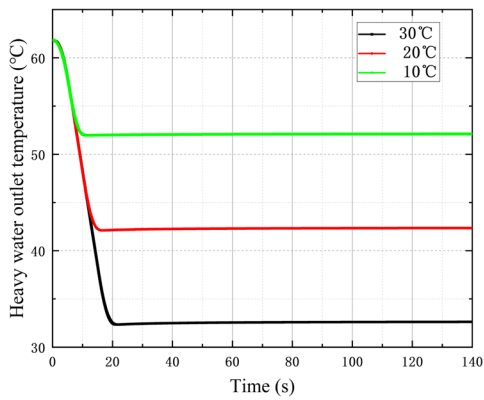
**Fig. 13** (Color online) Reactor response to a transient in which the heavy water inlet temperature decreased linearly by 20 °C



(a)



(b)



(c)

**Fig. 14** (Color online) **a** Power response, **b** fuel salt outlet temperature response, and **c** heavy water outlet temperature response to transients in which the heavy water inlet temperature decreased by 10 °C –30 °C

which the inlet heavy water temperature decreased by 10 to 30 °C. The transient with a larger decrease in the inlet heavy water temperature introduced a more positive reactivity to the core. This resulted in a higher core power, which subsequently led to a higher outlet temperature of the fuel salt. However, the increased core power and fuel salt temperature could not offset the effect of the heavy water temperature

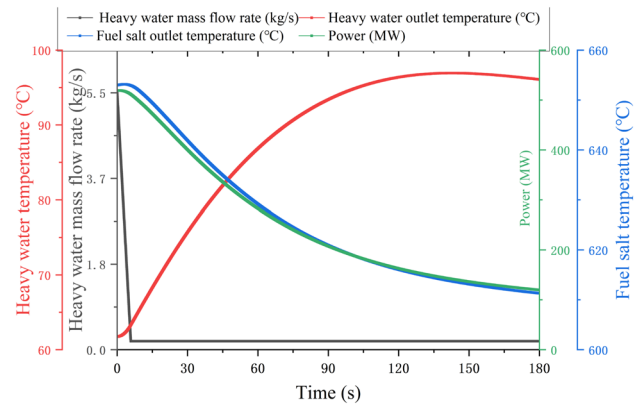


**Fig. 15** (Color online) Reactor response to a transient in which the heavy water mass flow rate decreased linearly from 100% to 3.3%

decrease caused by the decrease in the inlet heavy water temperature. This was owing to the extremely low thermal conductivity of the insulating layer and high heat capacity of heavy water. Consequently, the outlet temperature of the heavy water decreased with a decrease in the inlet heavy water temperature. To maintain the core temperature below 700 °C and ensure reactor safety, the decrease in inlet heavy water temperature should not exceed 40 °C.

For transients with increasing inlet heavy water temperature (< 100 °C at the inlet), the response of the reactor was inverted to that of the transients in which the inlet heavy water temperature decreased and did not endanger the core safety.

#### 4.5 Heavy water mass flow rate decrease

The mass flow rate of heavy water, which is similar to the flow rate of molten salt, plays a crucial role in reactor safety. If the heavy water pump fails or a pipe ruptures in the moderator cooling system, the mass flow rate of the heavy water decreases. A reduction in the mass flow rate of heavy water prolongs the residence time of heavy water in the core, leading to an increase in the heavy water temperature. This introduces a negative reactivity to the core and subsequently decreases the reactor power. The decreased power then results in a decrease in the molten salt temperature, which introduces a positive reactivity to the core and mitigates the decrease in core power. Figure 15 shows a transient in which the heavy water mass flow rate decreased linearly from 5.48 kg/s (velocity 0.6 m/s) to 0.18 kg/s in 5.8 s. The heavy water temperature increased significantly and subsequently introduced a negative reactivity to the core, causing a rapid decrease in the reactor power and molten salt temperature. The decreased fuel salt temperature, in turn, triggered a positive reactivity in the core, which slowed the decline rate of the reactor power and molten salt outlet temperature, and a

new steady state was reached. Both the decreased core power and molten salt temperature led to a marginal decrease in the heavy water outlet temperature after reaching its peak of (97 °C) at approximately 130 s.

Figure 16 shows the responses of core power and the outlet temperatures of fuel salt and heavy water to transients in which the inlet heavy water velocity decreased to 0.01 m/s  $-0.3$  m/s in 5.9 s–3 s, respectively. The transient with a larger decrease in the inlet heavy water resulted in a longer residence time in the core. This caused a more significant increase in the heavy water temperature, which resulted in larger decreases in the core power and fuel salt temperature. Notably, the physical properties of heavy water were assumed to remain constant after its temperature exceeded 100 °C to simplify the calculation. Therefore, to maintain the temperature of the heavy water below its boiling point and ensure the safety of the core, the inlet mass flow rate of the heavy water must not decrease lower than 0.18 kg/s.

## 5 Conclusion

In 2019, Wu et al. [19] proposed a novel MSR concept moderated by heavy water, i.e., the HWMSR, to address the limitations of conventional MSRs resulting from the application of graphite, such as positive temperature feedback and nuclear waste management. The core design and nuclear fuel cycle of HWMSR have been extensively studied; however, the safety of HWMSRs remains to be evaluated. Therefore, we conducted a preliminary safety study for an SM-HWMSR by analyzing typical transients specialized to HWMSRs. A transient analysis code, HWMSR-2D, was developed for the HWMSR based on the existing code, TMSR-2D, which was oriented for graphite-moderated MSRs. The steady state of the SM-HWMSR was then calculated to provide the initial conditions for the transient analysis. By referring to the typical transients of graphite-moderated MSRs and considering the application of heavy water, the transients induced by the abnormal temperatures and flow rates of fuel salt and heavy water, including the overcooling and overheating of inlet fuel salt, fuel salt flow rate decrease accidents, overcooling and overheating of inlet heavy water, and heavy water mass flow rate decrease, were chosen for analysis. In addition, we varied the transient conditions over a wide range to explore the safety limitations of each transient. The results indicated that decreases in fuel salt temperature, fuel salt flow rate, heavy water temperature, and heavy water mass flow rate should not exceed 540 °C and 660 °C, 60%, 40 °C and 100 °C, and 3.3% for the overcooling and overheating of inlet fuel salt, a fuel salt flow rate decrease accident, the overcooling and overheating of inlet heavy water, and a heavy water mass

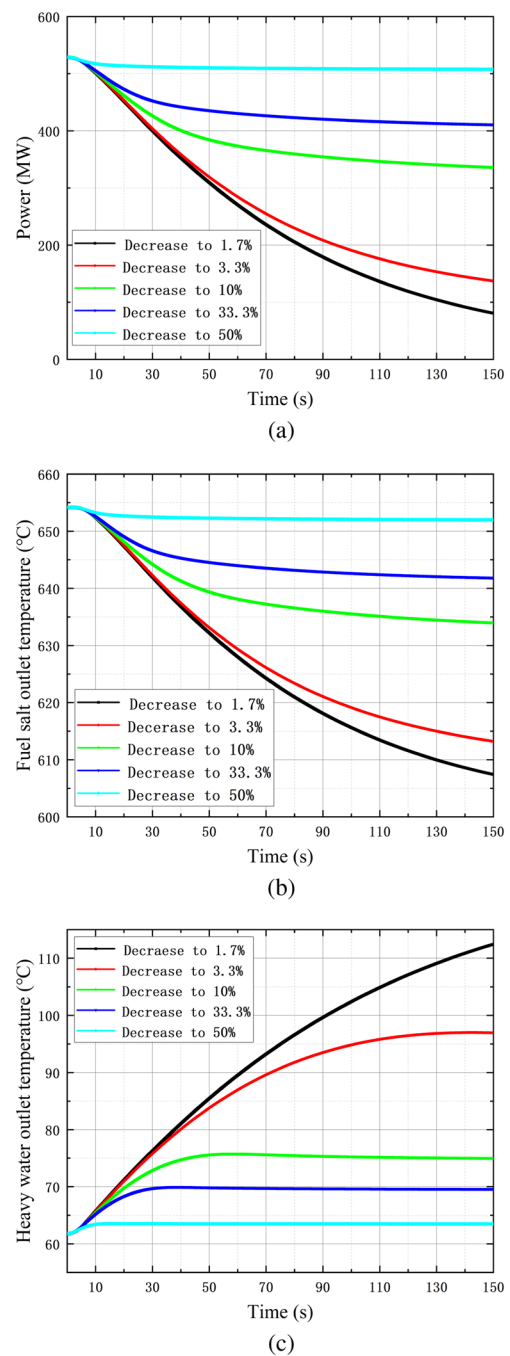


**Fig. 16** (Color online) **a** Power response, **b** fuel salt outlet temperature response, and **c** heavy water outlet temperature response to transients in which the heavy water mass flow rate decreased to 1.7–50%

flow rate decrease accident, respectively. Otherwise, severe accidents, including core meltdowns and heavy water vapor explosions, may occur.

However, the calculation results also demonstrated that all transients could reach a new stable state owing to the

negative temperature feedback, which could balance the increase in core power. Both the magnitude of the change and the balance time of the new steady state were determined by the extent to which the transient condition deviated from the initial condition. Compared with the transients resulting from abnormal changes in the fuel salt, the response of the core power and temperature to the transients driven by abnormal changes in heavy water was relatively slow, which allowed more time for the core to take action. This is also a notable advantage of using heavy water as a moderator. However, the calculations in this study did not consider the lateral flow of heavy water. Thus, further improvement in the calculation model is required in the future.

## 6 Options for future work and improvements

In the future, high-temperature moderators such as  ${}^7\text{LiOH}$  and  $\text{Mg}(\text{OD})_2$ , etc. can be explored to improve the concept of MSR. These moderators can operate at higher temperatures compared with heavy water, potentially enabling a more compact reactor with a reduced neutron slowing distance. Another issue is mitigating the neutron absorption of the thermal insulator composition of  $\text{Y}_2\text{O}_3$ . The use of a gas gap filled with  $\text{CO}_2$  or argon between the fuel channels and moderator would be an effective approach.

**Acknowledgements** The authors would like to express their appreciation to SINAP and CAS (Shanghai Institute of Applied Physics, Chinese Academy of Sciences) for providing computational codes. Gratitude is also extended to SINAP for their generous financial support, which has played a pivotal role in sustaining this study. We also extend our thanks to all those who supported and contributed to this study.

**Author Contributions** All authors contributed to the study conception and design. Directional guidance was provided by Xiang-Zhou Cai and Jin-Gen Chen, and code writing, data collection, and analysis were performed by Gao-Ang Wen, Jian-Hui Wu, and Chun-Yan Zou. The first draft of the manuscript was written by Gao-Ang Wen, and Man Bao providing collaboration. All authors commented on previous versions of the manuscript. All authors read and approved the final manuscript.

## Declarations

**Conflict of interest** The authors declare that they have no conflict of interest.

## References

- S. Jérôme, A. Michel, B. Ondřej et al., The molten salt reactor (MSR) in generation IV: overview and perspectives. *Prog. Nucl. Energ.* **77**, 308–319 (2014). <https://doi.org/10.1016/j.pnucene.2014.02.014>
- C. Zou, C. Cai, C. Yu et al., Transition to thorium fuel cycle for TMSR. *Nucl. Eng. Des.* **330**, 420–428 (2018). <https://doi.org/10.1016/j.nucengdes.2018.01.033>
- B. Olivier, B. Daniel, I. Evgeny et al., Overview of generation IV (Gen IV) reactor designs-safety and radiological protection considerations. (2012)
- P.N. Haubenreich, J.R. Engel, Experience with the Molten-Salt reactor experiment. *Nucl. Appl. Technol.* **8**, 118–136 (1970). <https://doi.org/10.13182/nt8-2-118>
- H. Xu, Z. Dai, X. Cai, An overview of the thorium program plan of the Chinese Academy of Sciences. *Trans. Am. Nucl. Soc.* **111**, 195 (2014)
- Q. Wei, L. Mei, Z. Zhan et al., Preliminary study on safety characteristics of molten salt reactor. *At. Energy Sci. Technol.* **48**, 2280 (2014). [\(in Chinese\)](https://doi.org/10.7538/yzk.2014.48.12.2280)
- C. Zou, X. Cai, D. Jiang et al., Optimization of temperature coefficient and breeding ratio for a graphite-moderated molten salt reactor. *Nucl. Eng. Des.* **281**, 114–120 (2015). <https://doi.org/10.1016/j.nucengdes.2014.11.022>
- K. Yang, W. Qin, J. Chen et al., Neutron excess method for performance assessment of thorium-based fuel in a breed-and-burn reactor with various coolants. *Nucl. Sci. Tech.* **27**, 99 (2016). <https://doi.org/10.1007/s41365-016-0096-4>
- X. Cai, Z. Dai, H. Xu, Thorium molten salt reactor nuclear energy system. *Phys. (in Chinese)* **45**, 578–590 (2016). <https://doi.org/10.7693/wl20160904>
- X. Li, J. Wu, C. Yu et al., Thorium utilization strategy for a small modular molten salt reactor. *Nucl. Phys. Rev.* **34**, 672–676 (2017). <https://doi.org/10.11804/NuclPhysRev.34.03.672>
- Y. Liu, R. Guo, X. Cai et al., Breeding properties study on high-power thorium molten salt reactor. *J. Nucl. Eng. Radiat. Sci.* **5**, 011003 (2019). <https://doi.org/10.1115/1.4041272>
- Y. Cui, J.G. Chen, J. Wu et al., Development and verification of a three-dimensional spatial dynamics code for molten salt reactors. *Ann. Nucl. Energy* **171**, 109040 (2022). <https://doi.org/10.1016/j.anucene.2022.109040>
- K. Nagy, J.L. Kloosterman, D. Lathouwers et al., The effects of core zoning on the graphite lifespan and breeding gain of a moderated molten salt reactor. *Ann. Nucl. Energy* **43**, 19–25 (2012). <https://doi.org/10.1016/j.anucene.2011.12.025>
- J.P. Carter, R.A. Borrelli, Integral molten salt reactor neutron physics study using Monte Carlo N-particle code. *Nucl. Eng. Des.* **365**, 110718 (2020). <https://doi.org/10.1016/j.nucengdes.2020.110718>
- Y. Liu, W. Li, R. Yan et al., Effect of FLiBe thermal neutron scattering on reactivity of molten salt reactor. *Nucl. EPJ Web Conf.* **239**, 14008 (2020). <https://doi.org/10.1051/epjconf/20203914008>
- X. Li, D. Cui, C. Zou et al., Assembly-level analysis on temperature coefficient of reactivity in a graphite-moderated fuel salt reactor fueled with low-enriched uranium. *Nucl. Sci. Tech.* **34**, 70 (2023). <https://doi.org/10.1007/s41365-023-01216-0>
- T.J. Dolan, *Molten salt reactors and thorium energy* (Woodhead Publishing, Sawston, 2017). <https://doi.org/10.1016/b978-0-08-101126-3.00027-0>
- H.R. Trellue, R.J. Kapernick, D.V. Rao et al., Salt-cooled modular innovative thorium heavy water-moderated reactor system. *Nucl. Technol.* **182**, 26–38 (2013). <https://doi.org/10.13182/nt13-a15823>
- J. Wu, J. Chen, X. Kang et al., A novel concept for a molten salt reactor moderated by heavy water. *Ann. Nucl. Energy* **132**, 391–403 (2019). <https://doi.org/10.1016/j.anucene.2019.04.043>
- J. Wu, J. Chen, C. Zou et al., Transition to thorium fuel cycle on a heavy water moderated molten salt reactor by using low

- enrichment uranium. *Ann. Nucl. Energy* **165**, 108638 (2022). <https://doi.org/10.1016/j.anucene.2021.108638>
21. J. Wu, C. Yu, C. Zou et al., Influences of reprocessing separation efficiency on the fuel cycle performances for a Heavy Water moderated Molten Salt Reactor. *Nucl. Eng. Des.* **380**, 111311 (2021). <https://doi.org/10.1016/j.nucengdes.2021.111311>
  22. J. Wu, C. Zou, C. Yu et al., Study of natural uranium utilization in a heavy water moderated molten salt reactor. *Prog. Nucl. Energy*. **146**, 104144 (2022). <https://doi.org/10.1016/j.pnucene.2022.104144>
  23. Y. Zhang, J. Wu, J. Chen et al., Ex-core transition to thorium cycle in a small modular heavy-water moderated molten salt reactor with unchanged concentration of heavy metal nuclides in the fuel salt. *Int. J. Energy Res.* **45**, 12383–12395 (2021). <https://doi.org/10.1002/er.6574>
  24. G. Zheng, H. Wu, J. Wang et al., Thorium-based molten salt SMR as the nuclear technology pathway from a market-oriented perspective. *Ann. Nucl. Energy* **116**, 177–186 (2018). <https://doi.org/10.1016/j.anucene.2018.02.004>
  25. Y. Zhang, Y. Ma, J. Wu et al., Preliminary analysis of fuel cycle performance for a small modular heavy water-moderated thorium molten salt reactor. *Nucl. Sci. Tech.* **31**, 108 (2020). <https://doi.org/10.1007/s41365-020-00823-5>
  26. C.K. Chow, H.F. Khartabil, Conceptual fuel channel designs for candu-Scwr. *Nucl. Eng. Technol.* **40**, 139–146 (2008). <https://doi.org/10.5516/net.2008.40.2.139>
  27. K. Sasaki, T. Terai, A. Suzuki et al., Effect of the  $Y_2O_3$  concentration in YSZ on the thermophysical property as a thermal shielding material. *Int. J. Appl. Ceram. Technol.* **7**, 518 (2009). <https://doi.org/10.1111/j.1744-7402.2009.02363.x>
  28. R.O. Scarlat, M.R. Laufer, E.D. Blandford et al., Design and licensing strategies for the fluoride-salt-cooled, high-temperature reactor (FHR) technology. *Prog. Nucl. Energy*. **77**, 406–420 (2014). <https://doi.org/10.1016/j.pnucene.2014.07.002>
  29. R.C. Robertson, Conceptual design study of a single-fluid molten-salt breeder reactor (1971). <https://doi.org/10.2172/4030941>
  30. J. Wu, J. Chen, X. Cai et al., A review of molten salt reactor multi-physics coupling models and development prospects. *Energies* **15**, 8296 (2022). <https://doi.org/10.3390/en15218296>
  31. Q. Wei, W. Guo, H. Wang et al., Develop and verify coupling program of the neutron physics and thermal hydraulic for MSR. *Nucl. Tech.* **40**, 100605 (2017). <https://doi.org/10.11889/j.0253-3219.2017.hjs.40.100605>. (in Chinese)
  32. Y. Cui, L. Cui, S.P. Xia et al., Dynamic analysis for a 2 MW liquid-fueled molten salt reactor. *Prog. Nucl. Energy*. **126**, 103381 (2020). <https://doi.org/10.1016/j.pnucene.2020.103381>
  33. Y. Cui, J. Chen, M. Dai et al., Development of a steady state analysis code for molten salt reactor based on nodal expansion method. *Ann. Nucl. Energy* **151**, 107950 (2021). <https://doi.org/10.1016/j.anucene.2020.107950>
  34. C. Yu, C. Zou, J. Wu et al., Development and verification of molten salt reactor refueling and reprocessing system analysis code based on SCALE. *At. Energy Sci. Technol.* **52**, 2136 (2018). <https://doi.org/10.7538/yzk.2018.youxian.0123>. (in Chinese)
  35. F. Zhu, J. Wu, C. Yu et al., Research on coupling of neutronics and thermal-hydraulics for fuel assembly of thorium molten salt reactor moderated by zirconium hydride rod. *At. Energy Sci. Technol.* **54**, 2063 (2020). <https://doi.org/10.7538/yzk.2019.youxian.0803>. (in Chinese)
  36. J. Krepel, U. Rohde, U. Grundmann et al., Dynamics of molten salt reactors. *Nucl. Technol.* **164**, 34–44 (2008). <https://doi.org/10.13182/nt08-a4006>
  37. X. Zuo, M.S. Cheng, Y.Q. Dai et al., Flow field effect of delayed neutron precursors in liquid-fueled molten salt reactors. *Nucl. Sci. Tech.* **33**, 96 (2022). <https://doi.org/10.1007/s41365-022-01084-0>
  38. L. Li, Z. Zhang, Research on transient flux distribution in parallel channels. *Nucl. Power Eng.* **31**, (2010). (in Chinese)
  39. G. Marleau, A. Hebert, R. Robert, A user guide for DRAGON Version 4. (2011)
  40. W.H. Sides, Control Studies of a 1000-Mw(e) MSBR. (1970) <https://doi.org/10.2172/4115415>

Springer Nature or its licensor (e.g. a society or other partner) holds exclusive rights to this article under a publishing agreement with the author(s) or other rightsholder(s); author self-archiving of the accepted manuscript version of this article is solely governed by the terms of such publishing agreement and applicable law.